

## Ultrahigh-Vacuum Reaction Apparatus to Study Synchrotron-Radiation-Stimulated Processes

S. Hirano,<sup>a</sup> A. Yoshigoe,<sup>a†</sup> M. Nagasono,<sup>b</sup> K. Mase,<sup>b</sup> J. Ohara,<sup>c</sup> Y. Nonogaki,<sup>b</sup> Y. Takeda<sup>d</sup> and T. Urisu<sup>b\*</sup>

<sup>a</sup>The Graduate University for Advanced Studies, Institute for Molecular Science, Myodaiji, Okazaki 444-8585, Japan, <sup>b</sup>Department of Vacuum UV Photoscience, Institute for Molecular Science, Myodaiji, Okazaki 444-8585, Japan, <sup>c</sup>Research Laboratories, DENSO Co. Ltd, 500-1 Minamiyama, Komenoki Nisshin-cho, Aichi-Ken 470-0111, Japan, and <sup>d</sup>Department of Materials Science and Engineering, Graduate School of Engineering, Nagoya University, Furo-cho, Chikusa-ku, Nagoya 464-8603, Japan. E-mail: urisu@ims.ac.jp

(Received 20 April 1998; accepted 4 September 1998)

An ultrahigh-vacuum reaction apparatus to study synchrotron-radiation-stimulated processes has been constructed and placed on beamline 4B of the synchrotron radiation storage ring (UVSOR) at the Institute for Molecular Science. The apparatus is designed so that multiple synchrotron radiation processes such as etching and chemical vapour deposition can be carried out successively without breaking the high vacuum. It is equipped with IR reflection absorption spectroscopy (IRRAS) apparatus and reflective high-energy electron diffraction (RHEED) apparatus for *in situ* observations. The basic parameters of the apparatus including etching and deposition rates have been measured. IRRAS using buried metal layer substrates has been confirmed to be a very useful method of analyzing the reaction mechanisms of the synchrotron-radiation-stimulated processes.

**Keywords:** synchrotron-radiation-stimulated processes; IR reflection absorption spectroscopy; etching; chemical vapour deposition; molecular beam epitaxy.

### 1. Introduction

All molecules and atoms exhibit strong absorption associated with electronic transitions in the vacuum ultraviolet (VUV) range. Synchrotron radiation can therefore be used to induce a variety of photochemical reactions which cannot be excited by other light sources such as lasers or discharge lamps. Applications of these synchrotron-radiation-stimulated photochemical reactions to material processes, such as synchrotron-radiation-stimulated etching and chemical vapour deposition (CVD), was first demonstrated about 13 years ago and since then many experimental studies have been carried out (Urisu *et al.*, 1991). These synchrotron-radiation-stimulated processes demonstrate several unique characteristics such as low temperature, low damage, low contamination, high spatial resolution owing to the short wavelength of the radiation, and reaction selectivity *via* excitation energy tuning. The combination of these features using synchrotron radiation is anticipated to realise novel nano-process technology in the future. Studies in the past decade have succeeded in

demonstrating the potential merits of synchrotron radiation photochemical reactions applied to semiconductor processes such as etching, CVD, surface cleaning or modification, and epitaxial growth. The interesting phenomenon of material selectivity in surface reactions (Urisu & Kyuragi, 1987) is considered to be unique to core electron excitations, although the mechanism is not yet fully understood. The disadvantages of the synchrotron radiation process are also becoming clearer. The rather low reaction rate is considered to make it difficult to apply to conventional large-scale integrated circuit (LSI) manufacture, although perhaps it is suitable for the nano-processes.

An ultrahigh-vacuum (UHV) reaction apparatus for synchrotron-radiation-stimulated processing has been designed so that multiple processes such as surface cleaning, CVD and etching can be successively treated without breaking the high vacuum. An optical system for IR reflection absorption spectrum (IRRAS) measurements and a reflection high-energy electron diffraction (RHEED) apparatus are installed for the *in situ* monitoring of the reaction. Experiments have been conducted at beamline 4B of the synchrotron radiation facility (UVSOR) of the Institute for Molecular Science to evaluate the basic performance of this apparatus.

† Present address: Department of Synchrotron Radiation Research, Japan Atomic Energy Research Institute, 323 Mihara, Mikazuki, Sayo, Hyogo 679-5143, Japan.

## 2. Design of the apparatus

The apparatus consists of four UHV chambers which are used for etching or surface modification reactions (ET), for epitaxial growth reactions (EP), for sample storage (ST) and as the air lock for the sample introduction (AL), as shown in Fig. 1. These are evacuated using  $300 \text{ l s}^{-1}$  (ET),  $50 \text{ l s}^{-1}$  (EP),  $150 \text{ l s}^{-1}$  (ST) and  $150 \text{ l s}^{-1}$  (AL) turbomolecular pumps (TMP), and the base pressure of the chambers (other than the AL chamber) is about  $1 \times 10^{-10}$  torr. The ET and EP chambers are equipped with IRRAS optical systems for the *in situ* observation of the vibrational spectra of the surface adsorbates. The RHEED gun is pumped by a  $150 \text{ l s}^{-1}$  TMP. The sample size is typically  $14 \times 14 \text{ mm}^2$ . The substrate temperature is monitored by a W–Re thermocouple gauge attached to the back of the sample and controlled *via* the current of the PG/PBN heater (pyrolytic graphite/pyrolytic boron nitride heater; Union Carbide Inc.). The regulated temperature ranges are 380–1300 K for the substrate in the EP chamber and 100–800 K in the ET chamber (which can be cooled by liquid nitrogen). The apparatus is connected to the synchrotron radiation beamline through the differential vacuum pumping chamber (DP) as shown in Fig. 1. The difference in pressure between the ET and DP chambers was observed as shown in Fig. 2. When the reaction gas pressure is high ( $>0.1$  torr), the etching experiments are conducted by closing the exhaust gate valve to save the reaction gas consumption. Data for the exhaust gate valve opened (open circles) and closed (closed circles) are compared in Fig. 2.

The IRRAS system is composed of a Fourier-transform IR spectrometer (FTIR; JEOR JIR-7000), six off-axis parabolic mirrors, a wire grid polarizer to select the p-polarization, and a mercury cadmium telluride (MCT) detector, and can monitor the reactions in the ET or the EP

chamber. The optical paths are purged with dry air without  $\text{CO}_2$ . For measurements in the ET chamber, a collimated parallel IR beam from the FTIR is focused on the sample surface at an incident angle of  $85^\circ$  by an off-axis parabolic mirror M2 (diameter  $D = 50 \text{ mm}$ , effective focus length  $F = 320 \text{ mm}$ , diverting angle  $\alpha = 65^\circ$ ) through a  $\text{BaF}_2$  window. The reflected beam is collimated again by mirror M5 ( $D = 50 \text{ mm}$ ,  $F = 320 \text{ mm}$ ,  $\alpha = 65^\circ$ ) and is focused onto the MCT detector by mirror M6 ( $D = 50 \text{ mm}$ ,  $F = 45 \text{ mm}$ ,  $\alpha = 90^\circ$ ). For measurements in the EP chamber, the IR beam is focused at an incident angle of  $82.5^\circ$  by mirror M4 ( $D = 50 \text{ mm}$ ,  $F = 320 \text{ mm}$ ,  $\alpha = 90^\circ$ ) through a  $\text{ZnSe}$  window. The reflected beam is collimated by mirror M7 ( $D = 50 \text{ mm}$ ,  $F = 320 \text{ mm}$ ,  $\alpha = 90^\circ$ ), and is focused onto the MCT detector by mirror M8 ( $D = 50 \text{ mm}$ ,  $F = 45 \text{ mm}$ ,  $\alpha = 90^\circ$ ). The signals from the MCT detector are amplified and produce IR spectra after fast FT calculation.

## 3. Buried metal layer substrate

IRRAS is a useful technique for the detection of the IR absorption of adsorbates on metal surfaces but it is largely ineffective when applied to semiconductor or insulator surfaces (Greenler, 1975; Hoffmann, 1983), although these are principal materials for semiconductor fabrication processes. However, we consider IRRAS to be an excellent method for the *in situ* monitoring of synchrotron-radiation-induced process reactions, which requires the introduction of an IR beam into the UHV chamber and high sensitive detection on the small area irradiated by the focused synchrotron radiation beam. To overcome this contradiction, a buried metal layer (BML) substrate, *i.e.* a substrate having a thin buried metal layer at a depth of 50–100 nm from the surface (Bermudez & Prokes, 1991; Ehrley

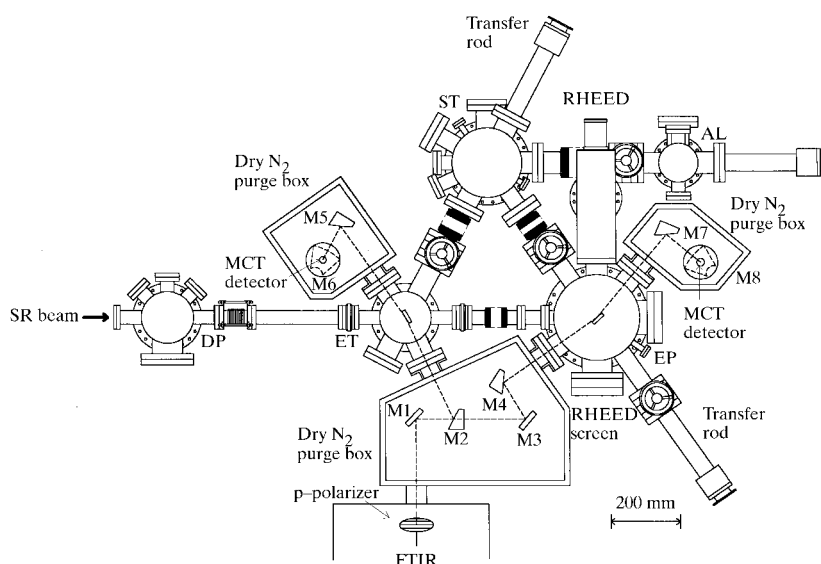


**Figure 1**

Reaction apparatus. AL, air-lock chamber for sample introduction; ST, sample storage chamber; ET, etching chamber; EP, epitaxial growth chamber; DP, differential vacuum pumping chamber; SR, synchrotron radiation. RHEED and IRRAS optical systems are attached for *in situ* observations. Characteristics of the mirrors M1–M8 and the turbomolecular pumps are given in the text.

*et al.*, 1991) is used in the IRRAS measurements. The surface of the BML substrate shows these characteristics of the surface materials for the chemical reactions but also reveals the characteristics of the buried metal, *i.e.* a high sensitivity for the p-polarized incident IR electromagnetic wave. In the present IRRAS observations, a  $\text{CoSi}_2$  Si(100) BML substrate was used. The structure and the fabrication process for the BML substrate is shown schematically in Fig. 3. The wafers after annealing [Fig. 3(c)] were purchased from Toray Research Centre Inc. The well defined epitaxial layer in Fig. 3(d) was formed by conventional gas-source molecular beam epitaxy (GS-MBE) using  $\text{Si}_2\text{H}_6$  in the EP chamber as described in §4.2. The fabrication process and the characterization of the surface of the  $\text{CoSi}_2$  BML substrate have previously been described in detail (Kobayashi *et al.*, 1996).

#### 4. Synchrotron radiation process experiments

Experiments on synchrotron-radiation-stimulated etching and Si GS-MBE have been conducted using the reaction apparatus shown in Fig. 1 on beamline 4B of UVSOR. The emitted beam from the storage ring is reflected and focused by the elliptically bent cylindrical mirror with a grazing incident angle of  $2^\circ$  and this is used to irradiate the substrate surface without monochromatization. The beam acceptance angles determined by this mirror are about 8 mrad (horizontal) and 4.2 mrad (vertical). The synchrotron radiation ring electron beam energy is 0.75 GeV and the beam current is 200 mA at injection and decreases to about 100 mA a few hours later. The beam spot sizes were  $12.6 \times 2.3 \text{ mm}^2$  (ET) and  $14 \times 3 \text{ mm}^2$  (EP) on the surface of the substrate, when they were set perpendicular to the beam. The calculated beam photon flux at 100 mA ring current is  $3.2 \times 10^{16} \text{ photons s}^{-1}$  (0.96 W), so the flux densities on the substrate surface are  $1.1 \times 10^{17}$  (ET) and

$7.6 \times 10^{16} \text{ photons cm}^{-2} \text{ s}^{-1}$  (EP) for an average ring current of 100 mA.

##### 4.1. Etching

It is known that  $\text{SiO}_2$  is etched by synchrotron radiation irradiation when exposed to  $\text{SF}_6$  gas (Urisu & Kyuragi, 1987). To test the performance of the present apparatus, synchrotron-radiation-stimulated etching of a 1.2  $\mu\text{m}$ -thick  $\text{SiO}_2$  film, which was grown by thermal oxidation on the Si(100) surface, was conducted using  $\text{SF}_6$  gas. The substrate was set perpendicular to the irradiation beam.

A 0.1 mm-thick stainless steel or a thin ( $\sim 38 \text{ nm}$ ) Al film deposited on the  $\text{SiO}_2$  surface was used as a contact etching mask for measuring the etching rate. These masks have a  $1 \times 1 \text{ mm}^2$  opening pattern. After a certain irradiation time under the reaction gas, the etched depth profile was measured by using the step profile meter. Figs. 4(a) and 4(b) show the etched patterns obtained (a) using the Al thin-film mask and (b) using the stainless steel mask, respectively, at an  $\text{SF}_6$  gas pressure of 0.05 torr. It must be noted that the low-etching-rate region appears close to the mask edge when using the stainless steel mask, while it was not observed in the Al contact mask independent of the conditions. At present, the reason for the appearance of the low-etching-rate region close to the edge of the thick mask is not clear. As a possible reason, we consider the shadow effects of the thick mask edge. The etching rate depends both on the surface intensity of the irradiation light and the surface density of the reaction precursors. If the thickness of the mask is larger than the mean free path of the gas-phase precursors, the surface density of the precursor is

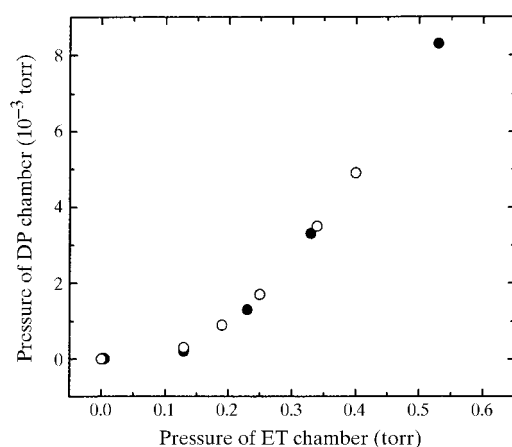


**Figure 2**

Relation between the DP chamber pressure (vertical axis) and the ET chamber pressure (horizontal axis), showing operation with the ET chamber exhaust gate valve open (open circles) and with the gate valve closed (closed circles).

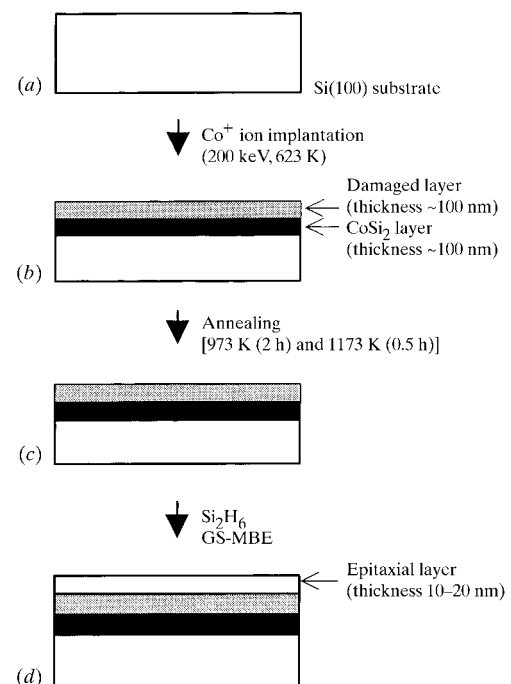


**Figure 3**

Fabrication process for the  $\text{CoSi}_2$  BML substrate.

considered to be low close to the mask edge due to the shadow effects. In reality, under high pressure (0.5 torr), which makes the mean free path of the precursor in the gas phase short, the low-etching-rate region almost disappears. To clarify this mask edge effect, more detailed experiments such as the detection of the surface precursor distribution are necessary. In the following, the etching rate observed by using the Al thin-film mask is discussed. Fig. 5 shows the observed dependence of the etched depth on the SF<sub>6</sub> gas pressure for an irradiation dose (ring current × irradiation time) of 10000 mA min. It is known that the rate increases with increasing pressure, then saturates or starts to decrease in the higher pressure region. This is because the synchrotron radiation beam is attenuated by the reaction gas absorption on the beam path in the high-pressure region. The maximum etching rate obtained was about 0.47 nm (100 mA min)<sup>-1</sup> at 0.05 torr. Next, the dependence of the etched depth on the irradiation dose was measured as shown in Fig. 6 at an SF<sub>6</sub> gas pressure of 0.05 torr. It is known that the depth increases linearly with increasing dose, *i.e.* the rate, about 0.47 nm (100 mA min)<sup>-1</sup>, is independent of the irradiation dose.

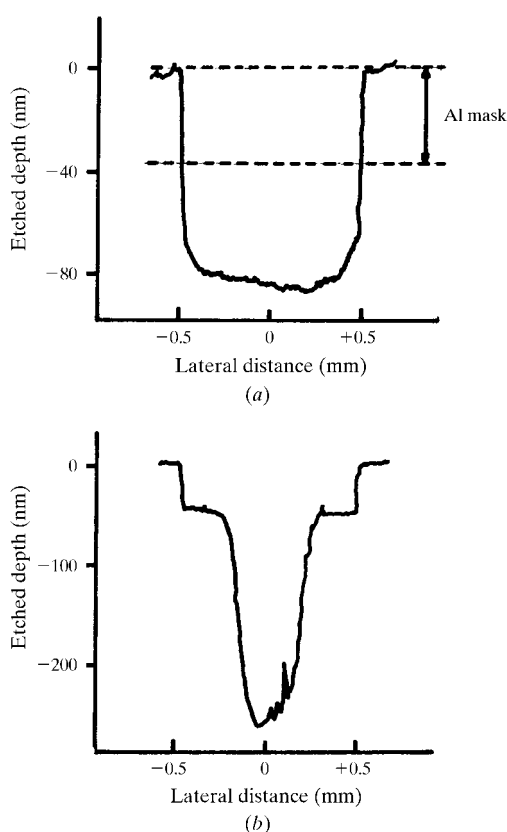


**Figure 4**

Depth profile of the etched pattern in SiO<sub>2</sub>. The reaction gas was SF<sub>6</sub> (0.05 torr). The exposure dose of the synchrotron radiation irradiation was 1 × 10<sup>4</sup> mA min. (a) An Al (thickness ~38 nm) contact mask with 1 × 1 mm<sup>2</sup> opening was used. (b) A stainless steel (thickness 0.1 mm) contact mask with 1 × 1 mm<sup>2</sup> opening was used.

#### 4.2. Epitaxial growth and in situ observation of surface hydrogen

The synchrotron-radiation-stimulated Si GS-MBE was examined using the EP chamber. Si<sub>2</sub>H<sub>6</sub> gas (1 × 10<sup>-3</sup> torr) was introduced into the EP chamber during synchrotron radiation irradiation at an incident angle of 45°. The observed deposition rate and the RHEED pattern, as a function of substrate temperature, are given in Table 1. The IRRAS measurements were carried out using the CoSi<sub>2</sub> BML substrate. The as-purchased CoSi<sub>2</sub> BML substrate [Fig. 3(c)] was cleaned using wet processes; namely, by dipping into a 3% HF solution for 30 s, dipping into a 4:1:1 HCl:H<sub>2</sub>O<sub>2</sub>:H<sub>2</sub>O solution for 10 min, and washing with deionized water. After drying using N<sub>2</sub> gas, the substrate was introduced into the EP chamber and then, after

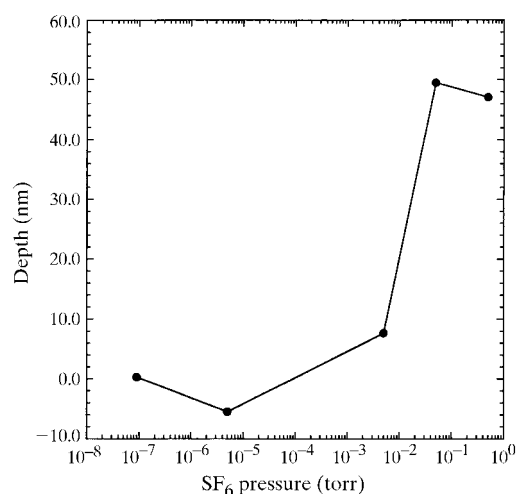


**Figure 5**

Dependence of the etched depth on the SF<sub>6</sub> gas pressure. The synchrotron radiation irradiation dose was 1 × 10<sup>4</sup> mA min. Observed values at 1 × 10<sup>-7</sup> torr and 5 × 10<sup>-6</sup> torr are within the measurement error (~±5 nm).

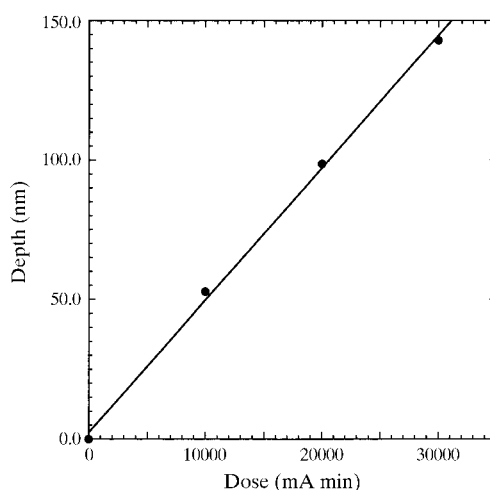


**Figure 6**

Dependence of the etched depth on the synchrotron radiation irradiation dose. The SF<sub>6</sub> gas pressure was 0.05 torr.

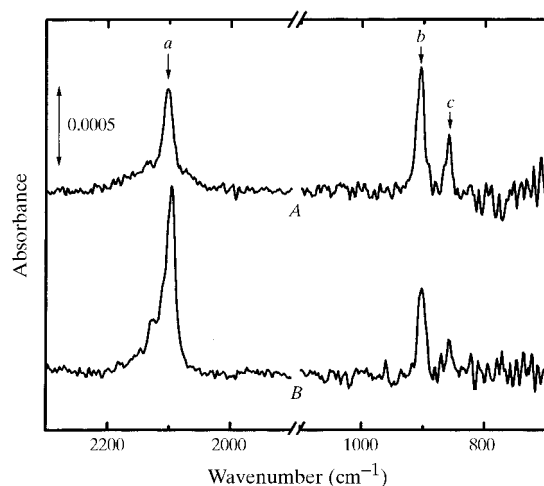
**Table 1**

The measured deposition rate and the RHEED pattern in the synchrotron-radiation-stimulated Si GS-MBE.

Si<sub>2</sub>H<sub>6</sub> gas pressure:  $1 \times 10^{-3}$  torr.

Substrate temperature (K)	Deposition rate [nm (100 mA min) <sup>-1</sup> ]	RHEED pattern
413	0.038	1 × 1
548	0.06	1 × 1
673	0.075	2 × 1
733	0.08	2 × 1
773	0.09	2 × 1
830	0.23	2 × 1

removing the thin surface oxide layer by heating to 1220 K, a well defined Si(100) layer of thickness  $\sim 10$  nm was deposited on the BML substrate surface by conventional thermal GS-MBE at 970 K using Si<sub>2</sub>H<sub>6</sub> [Fig. 3(d)]. This BML substrate, which had a well defined Si(100) layer on the surface, was used as a substrate of the IRRAS experiments. In Fig. 7, spectrum *A* shows the measured IRRAS spectra for the surface just after deposition at 400 K. The synchrotron radiation irradiation dose was 3000 mA min. The IRRAS spectrum for the Si<sub>2</sub>H<sub>6</sub> saturation adsorbed Si(100) surface at 400 K is shown in Fig. 7 for comparison (spectrum *B*). Peaks *a*, *b* and *c* are assigned to SiH symmetric stretching (2100 cm<sup>-1</sup>), SiH<sub>2</sub> scissoring (904 cm<sup>-1</sup>) and SiH<sub>3</sub> symmetric deformation vibration (858 cm<sup>-1</sup>) modes, respectively (Yoshigoe *et al.*, 1995). By comparing spectra *A* and *B* in Fig. 7 it can be seen that coverage by the higher Si hydrides species is much greater on the surface after epitaxial growth than on a surface obtained simply by chemisorbing Si<sub>2</sub>H<sub>6</sub>. In Fig. 8, the

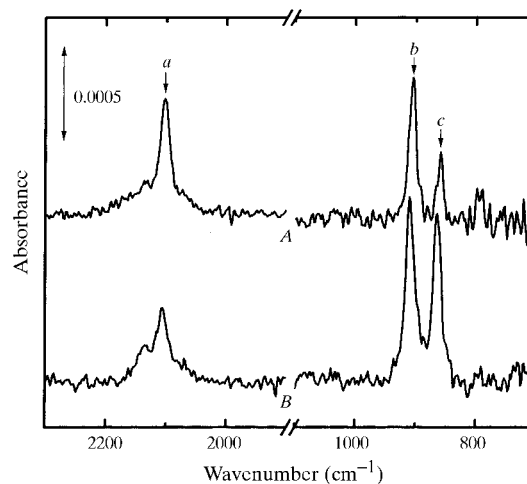
**Figure 7**

IRRAS spectra measured after synchrotron-radiation-stimulated Si GS-MBE (*A*) and after the saturation adsorption of Si<sub>2</sub>H<sub>6</sub> gas at 400 K (*B*). Synchrotron-radiation-stimulated Si GS-MBE was performed under an Si<sub>2</sub>H<sub>6</sub> gas pressure of  $1 \times 10^{-3}$  torr, with a substrate temperature of 400 K and a synchrotron radiation dose of 3000 mA min. A CoSi<sub>2</sub> BML substrate was used. Peaks *a*, *b* and *c* are assigned to SiH symmetric stretching, SiH<sub>2</sub> scissoring and SiH<sub>3</sub> symmetric deformation vibration modes, respectively.

IRRAS spectra in these two arrangements are compared; *i.e.* with the synchrotron radiation beam irradiating the substrate surface at an incident angle of 45° (*A*), and without irradiation, *i.e.* with the beam parallel to the substrate surface (*B*). It is shown from these results that the coverage by the higher Si hydrides species is much greater using the parallel arrangement (*B*). Therefore, from the data of Figs. 7 and 8, it is concluded that chemisorption of SiH<sub>2</sub> and SiH<sub>3</sub> generated in the gas phase by synchrotron radiation irradiation and the decomposition of these species on the surface by the synchrotron radiation irradiation is a key process in Si film growth. A detailed investigation of the deposition mechanism is not the aim of the present report. However, from these IRRAS data, we consider that the *in situ* observation by IRRAS is a powerful new technique for the study of the surface-reaction mechanism.

## 5. Summary

A UHV reaction apparatus for synchrotron-radiation-induced process experiments was constructed and set up on beamline 4B of the UVSOR storage ring. The chambers were designed so that multiple synchrotron radiation processes such as etching and CVD can be carried out successively without breaking the high vacuum. IRRAS and RHEED systems are installed for *in situ* observations of the surfaces. The basic parameters of the apparatus and etching and deposition rates have been measured. The usefulness of BML-IRRAS as an *in situ* observation technique for the study of surface reaction mechanisms has been clearly demonstrated.

**Figure 8**

IRRAS spectra after synchrotron-radiation-stimulated Si GS-MBE, with the synchrotron radiation beam irradiating the sample surface at an incidence angle of 45° (*A*), and without irradiation, *i.e.* with the synchrotron radiation beam parallel to the substrate surface (*B*). The GS-MBE conditions were the same as those of Fig. 7. Peaks *a*, *b* and *c* are assigned to SiH symmetric stretching, SiH<sub>2</sub> scissoring and SiH<sub>3</sub> symmetric deformation vibration modes, respectively.

The authors would like to thank the staff of the UVSOR facility for help during the course of these experiments. This work was supported partly by Grants-in-Aid for Scientific Research from the Ministry of Education, Science, Sports and Culture, and by Collaboration Program of the Graduate University for Advanced Studies.

## References

- Bermudez, V. M. & Prokes, S. M. (1991). *Surf. Sci.* **248**, 201–206.
- Ehrley, W., Butz, R. & Mantel, S. (1991). *Surf. Sci.* **248**, 193–200.
- Greenler, R. G. (1975). *J. Vac. Sci. Technol.* **12**, 1410–1417.
- Hoffmann, F. M. (1983). *Surf. Sci. Rep.* **3**, 107–192.
- Kobayashi, Y., Sumitomo, K., Probhakaran, K. & Ogino, T. (1996). *J. Vac. Sci. Technol.* **A14**, 2263–2268.
- Urisu, T. & Kyuragi, H. (1987). *J. Vac. Sci. Technol.* **B5**, 1436–1440.
- Urisu, T., Takahashi, J., Utsumi, Y. & Akazawa, H. (1991). *Appl. Organomet. Chem.* **5**, 229–241.
- Yoshigoe, A., Mase, K., Tsusaka, T., Kobayashi, Y., Ogino, T. & Urisu, T. (1995). *Appl. Phys. Lett.* **67**, 2364–2366.